Whole-Body MRI and Whole Body ^{123}I-MIBG scintigraphy: comparison in Lines and High Risk Neuroblastoma. A pilot study.

Catia Olianti (✉ catia.olianti@unifi.it)

University Hospital Careggi: Azienda Ospedaliero Universitaria Careggi   https://orcid.org/0000-0002-2349-2621

Anna Perrone

University Hospital Meyer: Azienda Ospedaliero Universitaria Meyer

Emanuele Neri

University of Pisa Department of Transaltional Research on new technologies in Medicine and Surgery

Dania Cioni

University of Pisa Department of Surgical Pathology Molecular Medicine of the Critical Area: Universita degli Studi di Pisa Dipartimento di Patologia Chirurgica Medica Molecolare dell'Area Critica

Michela Allocca

Brotzu Hospital: Azienda Ospedaliera Brotzu

Marco Di Maurizio

University Hospital Meyer: Azienda Ospedaliero Universitaria Meyer

Federica Carra

University Hospital Meyer: Azienda Ospedaliero Universitaria Meyer

Annalisa Tondo

University Hospital Meyer: Azienda Ospedaliero Universitaria Meyer

---

Abstract

Purpose: To assess agreement between ^{123}I-metaiodobenzylguanidine (MIBG) and Whole Body Magnetic Resonance Imaging with diffusion-weighted whole-body imaging with background body signal suppression (WB MRI-DWIBS) in High and Low, Intermediate risk neuroblastoma, a retrospective review was performed on MIBG and DWIBS paired scans acquired at diagnosis, response-to-therapy steps, after-surgery, off therapy.

Methods: 80 paired MIBG and DWIBS scans were acquired for 31 patients between June 2009 and June 2019 within 30 days, without intercurrent therapy. SIOPEN Semi-quantitative scoring systems for NB with 12 body sections was applied at whole body MIBG and WB MRI-DWIBS acquired to evaluate the disease extent. We evaluated specificity, sensitivity, overall accuracy, positive predictive value (PPV) and negative predictive value (NPV) of WB MRI-DWIBS respect MIBG scintigraphy considered as gold standard, and vice versa.

Results: DWIBS and MIBG images were concordant in 890 out of the 960 analyzed segments, with high agreement between the two techniques (kendal =0.85 P<0.0001 and Chi 536.5975 p<0.0001). Considering MIBG as gold standard, WB MRI-DWIBS overall accuracy was 93%, sensitivity 78%, specificity 95%, PPV 77% and NPV 96%. Otherwise, MIBG overall accuracy was 93%; sensitivity 77%; specificity 97%; VPP 78%; VPN 95%, considering DWIBS as gold standard. MIBG and WB MRI-DWIBS SIOPEN scoring resulted superimposable (Rho Spearman = 0,88, p < 0,0001).

Conclusions: DWIBS and MIBG images showed very high concordance. WB MRI may represent an alternative in weak-avid MIBG tumors and for follow up assessment. An integrated imaging model is proposed for HR, Low and Intermediate Risk protocols.

Introduction

Neuroblastoma (NB) is the most frequent extracranial solid tumor of childhood, representing 8 to 10 % of all cases of childhood cancer [1].

Overall survival for patients with low- and intermediate-risk neuroblastoma is excellent (greater than 90%), while overall survival for high-risk patients remains approximately 40% [2].

In recent years combined multi-treatments of High-Risk Neuroblastoma (HR-NB) and Low and Intermediate Risk Neuroblastoma (Lines) protocols have improved the prognosis and quality of life of patients.

About 80% of neuroblastoma are metastatic (stage IV) at the time of presentation and metastasis are most commonly present at cortical bone and bone marrow: at diagnosis is crucial the identification of metastatic sites to evaluate the good response to treatment-

The specificity of ^{123}I-MetalodoBenzylGuanidine (MIBG) for detecting primary and secondary neuroblastoma has always been estimated close to 100%, while the sensitivity is 90-95% [3]. More recently was found in neuroblastoma that 123I-MIBG has a sensitivity of 88%–93% and a specificity of 83%–92% [4,5].

So, the guidelines recommend the use of Whole Body (WB) MIBG scintigraphy to assess the extent of the disease and according to the International Neuroblastoma Risk Group Staging System (INRGSS) the scintigraphic uptake in the skeleton is a condition for considering a patient to be a stage M [6]. Radioiodine-labeled MIBG is used to detect primary tumors and is the test of choice for identification of metastatic sites [5,7-10]. The addition of single photon emission computed tomography (SPECT) and SPECT/computed tomography to 123I-MIBG planar images can improve identification and characterization of sites of uptake [11].

Nevertheless, MIBG scintigraphy has some drawbacks as the radiation exposure, the weak or absent MIBG avidity in a 10% of neuroblastoma [4,5] and the suboptimal detection of small subcentimeter lesions [12,13].

Whole-body magnetic resonance imaging (WB MRI) has been used for evaluation of skeletal lesions, both for staging and follow-up in various oncologic diseasess, without the exposure of the patient to ionizing radiation [14].
To our knowledge, few series have been published about the diagnostic performance of WB-MRI in patients with neuroblastoma [15,16] compared to MIBG scintigraphy.

In 2012, in a case report, Pai Panandiker et al. compared MIBG scintigraphy with WB MRI with Diffusion-Weighted Imaging with background body signal Suppression (WB MRI-DWIBS) and proposed WB MRI for detecting small metastasis of neuroblastoma [17].

Recently, Ishiguchi et al. evaluated diagnostic performance of WB MRI-DWIBS and ^{18}F-FDG PET/TC for detecting lymph node and bone metastasis in pediatric patients with neuroblastoma [18].
However, to date, no large series have been published in which the usefulness of WB MRI to assess the skeletal tumor burden of neuroblastoma in comparison with MIBG scintigraphy, considered as the reference standard, was evaluated.

Aim of this pilot study is to assess the agreement between MIBG WB scintigraphy and WB MRI with DWIBS for detecting bone metastasis in high and intermediate risk neuroblastoma (NB), in order to improve and integrate metabolic nuclear medicine data in almost all diagnostic-therapeutic steps of metastatic neuroblastoma protocols.

Materials And Methods

Patient population

We retrospectively evaluated 31 patients (mean age: 6.46 ± 12.05 years; range 3 months -16 years and 4 months; 21 males, 10 females) with high risk-NB (19 HR-NB, 61%) and intermediate risk NB (12 L2-NB, 39%); four patients had relapse with metastatic skeletal involvement after completed standard diagnostic-therapeutic protocol HR-NB and Lines.

A total amount of 82 paired whole body and SPECT MIBG and WB-MRI/DWISB scans were acquired between June 2009 and June 2019 within 30 days, without intercurrent therapy. Two couple MIBG scintigraphy and WB MRI-DWIBS were rejected because of intercurrent CH-therapy: therefore, our data set included 80 paired WB MIBG scintigraphy – WB MRI-DWIBS. Two expert Nuclear Medicine Physicians (more than 10-20 year of activity) and two expert Radiologists (more than 5-10 year of activity) performed the readings of WB-scans on the basis of International Society of Pediatric Oncology Europe Neuroblastoma SIOPEN scoring system.

This retrospective study had institutional review board approval; written informed consent was obtained from all Parents or Guardians.

Whole-Body 123I-MIBG scintigraphy

All diagnostic MIBG scans were performed on the basis of 2002-2018 guidelines for scintigraphic examinations of NB [11,12,19]. Each patient received a ^{123}I-MIBG dose activity in accordance with European Association of Nuclear Medicine (EANM) dosage calculator [20,21], 5.18 MBq/kg was administered, with a maximum dose of 185 MBq (most of patients had a weight under 25 Kg, one has a weight of 38Kg with a maximum activity administered 236 MBq). All of them underwent to thyroid tissue iodine prophylaxis with Lugol's solution 5%, range 8-40 drops on the basis of weigh and age [19]. Whole Body vertex-feet and SPECT thoracic-abdominal tract images were acquired at about 24 hours, the first performed with 5-7 cm/min. bed velocity or 400 Kcounts for each spot scans 128x128 matrix; the second with shoot and stop 3degrees projections 20-30 sec./step, according to EANM GL 2010 [20], 20 patients on a Picker Philips Medical System and 11 patients more recently on a SIEMENS ECAM Gamma-camera, both equipped with MEGP parallel hole collimator.

All scintigraphic scans were acquired after voiding and for younger than three years children after voiding and diaper change. No patient needed a catheterization, only one had a catheter for clinical reasons. No patients underwent sedo-analgesia procedure, in last two years some of younger and less compliant patients had premedication with 1-3 mg of melatonine per os one hour before scan to induce a transient para-physiological sleep or a more relaxed state. Melatonine was useful in our own experience but a wider feasibility should be yet assessed. Most of the other children performed scans asleep at the presence of parents with entertainment methods (tablet with cartoons or baby-songs).

SIOPEN Scoring System

According to the SIOPEN semiquantitative scoring method, the skeleton was divided into 12 anatomical body segments as follows: the skull, the thoracic cage, the proximal right upper limb, the distal right upper

limb, the proximal left upper limb, the distal left upper limb, the spine, the pelvis, the proximal right lower limb, the distal right lower limb, the proximal left lower limb and the distal left lower limb. The extent and pattern of skeletal MIBG involvement was scored using a 0-6 scale to discriminate between focal discrete lesions and patterns of more diffuse infiltration [21-23]. As known this method define lesion extension with a 0-6 grade scoring: 0 no sites per segment, 1 one discrete site per segment, 2 two discrete sites per segment, 3 three discrete lesions, 4 more than three discrete foci or a single diffuse lesion involving <50% of the segment, 5 diffuse involvement of 50–95% of the segment, and 6 diffuse involvement of the entire segment (Fig.1, Tab.1) [24]. SPECT acquisition is usually useful in evaluation of difficult to read body segments i.e. neck, abdomen and spine for physiological superimposing images (salivary glands, activated brown fat, intestinal and bladder content, hepatic or spleen physiological activity close to adrenals) [5]. So, this scan, always performed in thoracic-abdomen district, was used to confirm MIBG-WB metabolic alterations and for controversial founding.

Whole Body MRI with Diffusion-weighted imaging with background body signal suppression (WB MRI-DWIBS)

MR examination was performed using a 1.5 or 3T scanner (Achieva and Achieva D-Stream, respectively; Philips Medical Systems, The Netherland) with patient in supine feet-first position; 58 exams were performed on 1.5T scanner and 22 exams on 3T equipment. Whole-body images were obtained with three or more consecutive package acquisitions, depending on body height, using Q-body coil for signal receiving and transmitting. The imaging protocol consisted of a coronal T2-weighted short time inversion-recovery (T2W-STIR) and axial diffusion weighted imaging with background body signal suppression (DWIBS) sequence. DWIBS was acquired using a short TI inversion recovery echo-planar imaging (STIR-EPI) sequence under free breathing applying one b-value (800 and1000 s/mm2 respectively for 3T and 1,5T scanner) in 62 exams and four b-value (0, 100, 200 and 800 s/mm2) in 18 cases performed on 3T scanner.

Multiplanar reconstructions (MPR) images and high-resolution maximum intensity projection (MIP) images were reconstructed in all cases.

Total acquisition time for whole-body MRI was approximately 45-50 minutes.

Younger or uncooperative children underwent general inhalation anesthesia with maintenance of spontaneous breathing and monitoring of vital parameters (heart rate, respiratory rate, SpO_2, $EtCO_2$), during performing MR examinations, in the presence of the anesthetist.

WB MRI Image analysis

Whole-body MRI data sets were transferred to a Picture Archiving and Communications System (PACS). Two independent radiologists with 10 and 5 years of WB MRI experience, respectively, blinded to 123I-MIBG scintigraphy, evaluated in consensus MR images. On MR images bone marrow involvement was considered positive if present abnormal and/or focal increase of DWIBS and/or STIR intensity not from

normal anatomic structure; DWIBS was evaluated only visually, in comparison with signal intensity of skeletal muscle. Quantitative analysis of ADC value (ADC, apparent diffusion coefficient) was not performed in this study. In case of discrepancies between STIR and DWIBS images, we considered as "true" DWIBS results.

SIOPEN scoring System was also applied to all WB MRI-DWIBS scans using the same scintigraphic criteria.

Statistical analysis

Specificity, sensibility, overall accuracy, VPP and VPN of WB MRI were estimated respect MIBG considered as gold standard. We performed furthermore the same analysis taking WB MRI-DWIBS as gold standard. Chi-square, parametric and not-parametric correlations were used to assess agreement degree among total scoring value, number of lesions, mean of scoring for each segment. T di Student for coupled data and mean comparison were used to compare mean±SD and % of segments resulted site of lesions among 80 paired data. $p < 0.05$ is considered as significative. Comparison between means for scoring data in pathological segments was studied with the Kendal-coefficient concordance and the sign-test. Wilcoxon test was used to compare the % of segments resulted as pathological.

Results

WB MRI-DWIBS and MIBG scoring evaluations were concordant in 890 out of the 960 analyzed segments: 769 negative concordant sites (80,1 %), 121 positive concordant (12,6 %); 36 DWIBS positive but MIBG negative sites (3.7%), 34 DWIBS negative but MIBG positive sites (3.5%), with high agreement between the two diagnostic techniques (κ = 0.85, P<0.0001 and Chi-square statistic 536.5975, p<0.00001). Example of concordant sites is shown in Fig 2. Images of discordant cases with false-positive WB-MRI are shown in Fig 3, while false-negative MIBG scintigraphy images in one case of weak avid neuroblastoma at onset is shown in Fig. 4. We report another discordant case with weak not homogeneus MIBG uptake in thoracic primary tumor and a focal intense alteration on dorsal spine, not clearly visible detected at DWIBS images (Fig.5).

If we consider MIBG as gold standard, WB MRI-DWIBS overall accuracy was 93%, sensitivity 78%, specificity 95%, PPV 77% and NPV 96%. Otherwise, if we consider WB MRI-DWIBS as gold standard, MIBG overall accuracy was 93%, sensitivity 77%, specificity 97%, PPV 78% and NPV 95%. Thus, MIBG and WB MRI SIOPEN scoring resulted superimposable (Rho Spearman = 0,88, p < 0,0001). (Tab.2)

Mean scoring value for MIBG and DWIBS in whole cohort of patients was 4.54±12 mean ±SD for MIBG and 4.64±9 mean ±SD for WB MRI DWIBS, with median value 0 (51%) and range 0-45 and median value 0 (57%) and range 0-42 respectively; considering only the pathologic segments we found 9.31±12 mean ±SD for MIBG and 10.91±12 mean ±SD for WB MRI-DWIBS with a median value 4 and range 1-45 and median value 6 and range 1-42 respectively. (Tab. 3)

If we consider the total number of lesions for MIBG and WB MRI-DWIBS we found in the whole cohort of patients the mean value of 5.25±9 mean ±SD for MIBG and 5.49±12 mean ±SD for WB-MRI/DWIBS, with median value 0 (51%) and range 0-56 and median value 0 (57%) and range 0-60 respectively; if we consider only the pathologic segments we found 10.8±16 mean ±SD for MIBG and 12.91±16 mean ±SD for WB-MRI with a median value 3 and range 1-56 and median value 5 and range 1-60 respectively. (Tab. 4)

Both parametric and not-parametric tests for paired data showed a very good concordance between MIBG and DWIBS: for mean scoring values was found a Pearson correlation R value of 0.81 and a Rho Spearman value of 0.97, $p < 0.0001$; for total number of lesions in whole population R 0.78 and Rho 0.97, $p < 0.0001$; only in pathologic segments, mean scoring value correlation had R 0.82 and Rho 0.97, $p < 0.0001$, and R 0.78 and Rho 0.96 $p < 0.0001$ for total number of lesions.

The comparison of paired data mean-scoring per-segment and % of segments, resulted site of disease, didn't show any significant difference: $t = 0.62$ with $p = 0.54$ for mean-scoring and $t = 0.46$ with $p = 0.65$ for % of pathologic segments. Non-parametric test, (Kendal-coefficient concordance) K= 0.76; sign-test =1. Wilcoxon test for % of pathologic segments $p = 0,61$ and for mean-scoring $p = 0,66$.

Discussion

MRI is an effective method for imaging neuroblastoma [25]. It shows high sensitivity in detecting bone marrow metastases, high intrinsic soft tissue contrast resolution, precise definition of intraspinal tumor extension, good delineation of diaphragmatic involvement of thoracic tumors [26,19]. WB MRI may represent a radiation-free alternative in the assessment of patients with NB and its feasibility has already been demonstrated for the work-up of oncologic patients with various neoplastic diseases, (e.g., melanoma, breast, colorectal, prostate cancers) or for hematologic diseases with nodal or bone marrow involvement (lymphoma, multiple myeloma) [27, 28].

WB MRI uses both conventional sequences which provide predominantly anatomical information, such STIR e T1 weighted sequences, and functional sequences, such DWI and/or DWIBS. As known, DWIBS is a particular DWI technique that provide functional information from entire body during free breathing, in high signal-to-noise ratio (SNR) images, leading to easy identification of small lesions and thereby helping to visualize the spread of the disease [29].

In particular, as regards neuroblastic tumors, DWI sequence, based on ADC maps, has been shown to be able to distinguish between benign and malignant neuroblastic tumors, and to be useful in evaluating the response to chemotherapy [30-33].

In the present study, we evaluated the diagnostic accuracy of WB MRI-DWIBS in the assessment of the burden of disease, compared to MIBG WB Scintigraphy considered as gold standard, applying SIOPEN scoring system to both methods. The SIOPEN scoring systems have been used in large international

clinical trials, showing to provide important prognostic information that can be used to guide appropriate therapy [34].

Our study demonstrates a good concordance about diagnosis, response to therapy and stop therapy evaluation scored by SIOPEN system on MIBG WB Scintigraphy and WB MRI-DWIBS. The two diagnostic techniques showed a high agreement of 92.7% of segments evaluated (80,1% negative concordant sites and 12.6% positive concordant sites) and resulted discordant in only 7.2% of segments evaluated (3.5% DWIBS negative but MIBG positive sites and 3.7% DWIBS positive but MIBG negative sites). Both mean scoring values for positive segments and percentage of segments appear superimposable, with few light differences of performance and high Rho Spearman value.

The scoring evaluation shows in our court of segments about a 20% of metastatic involvement in bone marrow for skull, thorax, spine, pelvis, femur and tibia, less percentage for the other sites.

Most of few discordant results regards skull, thorax and pelvis (slightly more sensitivity of MIBG), spine and limbs (slightly more sensitivity of MRI). As for ribs and skull, the lower sensitivity of WB MRI might be explained by thin thickness of these bones; to overcome the weakness on this segment we could perform as additional sequence an axial STIR sequence with thin thickness.

WB MIBG and WB MRI had high statistically significant agreement. Thus, if we consider MIBG as gold standard, WB-MRI overall accuracy is 93%, sensibility 78%, specificity 95%, VPP 77% and VPN 96%. Otherwise, if we consider DWIBS as gold standard, MIBG overall accuracy is 93%; sensibility 77%; specificity 97%; VPP 78%; VPN 95%. Thus, MIBG and WB-MRI SIOPEN scoring resulted superimposable (Rho Spearman = 0,88, p < 0,0001) with a light prevalence for MRI for sensibility and a light prevalence for MIBG about specificity as well known in clinical practice.

Also, the mean value of scoring for each segment shows a light prevalence of WB MRI on WB MIBG because of the higher sensibility on smaller signal-alterations related to the different resolution of two diagnostic method: about 7 -10 mm for MIBG [13] and about 4 mm for MRI [28]. Our data confirm also the assessment that MIBG scintigraphy is the best established and most widely used scintigraphic technique in the evaluation of NB because of its high sensitivity (97%) and specificity (83%-92%) [26]. A combination of MRI and MIBG scintigraphy has been shown to achieve the best sensitivity and specificity in NB imaging [19].

However, scintigraphy exposes patients to ionizing radiation. This is a major concern in children, who are at higher risk because of their smaller body size, higher mitotic rate, and longer life expectancy [35], in particular for low and intermediate risk NB.

According to protocol HR-NB, at least 7 MIBG- scintigraphy are necessary during the different steps of therapy with a high number of diagnostic examinations, and increased risk of potential secondary malignancies [11,35]. Leverdiere et al. found that the cumulative incidence of second malignant neoplasms in long survivor of neuroblastoma was 3.5% at 25 years and 7.0% at 30 years after diagnosis.

Compared with the sibling cohort, survivors had an increased risk of selected chronic health conditions (risk ratio [RR] = 8.3; 95% CI = 7.1 to 9.7) with a 20-year cumulative incidence of 41.1%. Endocrine complications are prevalent in childhood cancer survivors, with 50% experiencing at least one hormonal disorder over the course of their lives [36,37]. Moreover, Mostoufi et al. demonstrated at least one (16.7%) at least two (8,6%) and three or more (6.6%) endocrinopathies in survivors of neuroblastoma (31.9%) [38].

At our knowledge no other published study exists designed to perform a systematic comparison of SIOPEN Scoring on WB MIBG scintigraphy and on WB MRI-DWIBS. This may represent an important innovation about diagnostic evaluation and semiquantitative scoring of HR-NB and Intermediate-Risk NB. In our experience, the clinical introduction of WB MRI may be useful in diagnostic protocol of NB with very high accuracy in disease extension and functional complemental characterization of primary tumor and metastasis. This is even more important for those cases with weak or poor MIBG avidity, due to the degree of undifferentiation of tumor cells, as well as for neuroblastoma with loss of MIBG avidity at relapse, as demonstrated in two case of our series [15]. Also, in our experience, a combination of MRI and MIBG scintigraphy showed to achieve the best sensitivity and specificity in NB imaging.

As known, a limitation of WB MRI is the light overestimation of bone lesions, especially in post-chemotherapy examinations. At the onset, the false-positive findings at DWIBS sequences are often due to the high signal of the regions rich in red bone marrow in the normal developing skeleton, above all in lumbar spine and pelvic skeleton as reported by Muller et al [39]. Therefore, the radiologist experience is fundamental in the identification of these areas of physiological hyper-intensity.

WB MRI shows lightly less specificity compared to MIBG scintigraphy also during the evaluation of therapy response as it arises from our results, whose statistical analysis we have not reported because they are not reliable given the too small number of tests. This limit of DWIBS sequence can be explained in part by the so-called "T2 shine-through" phenomenon: high signal on diffusion-weighted images is not due to restricted diffusion, but rather to high T2 signal which 'shines through' to the DWI image. It can be overcome by evaluating the apparent diffusion coefficient (ADC), a value that measures the effect of diffusion independent of the influence of T2 shine-through [40], but our study lacks a quantitative analysis. Nevertheless, there are no validated bone ADC criteria in the literature, and there is a poor reproducibility of ADC measurements especially if the regions examined are "small". Furthermore, it should be added that especially in the evaluation of bone marrow there is a need to consider how the different types of treatment (chemotherapy, radiotherapy, immunotherapy) can affect the modification of the bone marrow signal intensity, data to date not yet clearly known [41,42]. These could be other interesting items for further studies.
An important limitation is given by the lack of a standardized technique in the execution of the WB MRI, with different protocols among the numerous published studies. Another weakness is the non-capillary diffusion of MRI instrumentation. Finally, the necessity of general inhalation anesthesia for less than four years old patients or for not collaborative ones, with the assistance of the pediatric anesthetist might be another limitation of MRI application. This is otherwise true also for scintigraphic acquisitions in particular for SPECT-CT modality.

Conclusions

WB MRI-DWIBS and WB MIBG scintigraphy can be considered as complementary tools in the evaluation of metastatic NB at the diagnosis and during the various steps of therapy. We propose an integrated diagnostic model where WB MRI-DWIBS could avoid the necessity or MIBG scan in some of multiple steps of HR and reduce thus the number of diagnostic MIBG scans in the course of HR and low and intermediate risk NB protocol. We usually perform both exams at staging, post-induction, post-surgery, before maintenance and at the end of treatment; in the steps post-high dose chemotherapy MIBG could be omitted in case of stable negativity of WB MRI-DWIBS. WB MRI assessment could be useful without any other diagnostic modality during the follow up: 123I-MIBG scan should be performed to confirm or exclude relapse, for the eventual restaging, and for metabolic typification of skeletal or soft tissue new lesions. Another possible employment of WB MRI imaging is relative to children with instable systemic onset of neuroblastoma, who need a staging assessment into a short time interval, WB MRI could allow both an evaluation of primary tumor with focused sequences and an evaluation of skeletal and extra-skeletal metastases, in a single exam without radiation exposure. Thus, as already affirmed a good combination of MRI and MIBG scintigraphy allows to achieve the best sensitivity and specificity in NB imaging.

Declarations

Funding: this study wasn't funded.

Conflict of Interest: Author Catia Olianti declares that she has no conflict of interest. Author Anna Perrone declares that she has no conflict of interest. Author Emanuele Neri declares that he has no conflict of interest. Author Dania Cioni declares that she has no conflict of interest. Author Michela Allocca declares that she has no conflict of interest. Author Marco Di Maurizio declares that he has no conflict of interest. Author Federica Carra declares that she has no conflict of interest. Author Annalisa Tondo declares that she has no conflict of interest.

Availability of data and material (data transparency) : the Authors give their availability.

Ethics approval: All procedures performed in studies involving human participants were in accordance with the ethical standards of the institutional and/or national research committee and with the 1964 Helsinki declaration and its later amendments or comparable ethical standards.

Informed consent: Informed consent was obtained from all individual participants included in the study.

Consent to participate: Author Catia Olianti allows participation. Author Anna Perrone consents the participation. Author Emanuele Neri allows participation. Author Dania Cioni allows participation. Author Michela Allocca allows participation. Author Marco Di Maurizio allows participation. Author Federica Carra allows participation. Author Annalisa Tondo allows participation.

References

1. Park JR, Eggert A, Caron H. Neuroblastoma: biology, prognosis, and treatment. Hematol Oncol Clin North Am 2010;24(1):65–86.

2. Wilson LM, Draper GJ. Neuroblastoma, its natural history and prognosis: a study of 487 cases. British medical journal. 1974; 3(5926):301-7.

3. Jacobs A, Delree M, Desprechins B, et al. Consolidating the role of ^{123}I-MIBG-scintigraphy in childhood neuroblastoma: five years of clinical experience. Pediatric radiology. 1990; 20(3):157-9.

4. Vik TA, Pflugger T, Radota R et al. 123I-MIBG scintigraphy in patients with known or suspected neuroblastoma: results from a prospective multicenter trial. Pediatr Blood Cancer 2009;52(17):784-790

5. Liu B, Zhuang H, Servaes S. Comparison of [123I]MIBG and [131I]MIBG for imaging of neuroblastoma and other neural crest tumors. Q J Nucl Med Mol Imaging 2013;57 (1):21–28.

6. Monclair T, Brodeur GM, Ambros PF, Brisse HJ, Cecchetto G, Holmes K, Kaneko M, London WB, Matthay KK, Nuchtern JG, von Schweinitz D, Simon T, Cohn SL, Pearson AD; INRG Task Force. International NB risk group (INGR) staging system: an INGR task force report. J Clin Oncol. 2009; 27: 298-303

7. Brodeur GM, Pritchard J, Berthold F, et al. Revisions of the international criteria for neuroblastoma diagnosis, staging, and response to treatment. J Clin Oncol 1993;11(8): 1466–1477.

8. Sharp SE, Trout AT, Weiss BD, Gelfand MJ . MIBG in Neuroblastoma Diagnostic Imaging, and Therapy. Radiographics Jan-Feb 2016;36(1):258-78. doi: 10.1148/rg.2016150099.

9. Brisse HJ, McCarville MB, Granata C, et al. Guidelines for imaging and staging of neuroblastic tumors: consensus report from the International Neuroblastoma Risk Group Project. Radiology 2011;261(1):243–257

10. Matthay KK, Shulkin B, Ladenstein R, et al. Criteria for evaluation of disease extent by 123I-metaiodobenzylguanidine scans in neuroblastoma: a report for the International Neuroblastoma Risk Group (INRG) Task Force. Br J Cancer 2010;102(9):1319–1326

11. Olivier P, Colarinha P, Fettich J, Fischer S, Frökier J, Giammarile F, Gordon I, Hahn K, Kabasakal L, Mann M, Mitjavila M, Piepsz A, Porn U, Sixt R, van Velzen J. Guidelines for radioiodinated MIBG scintigraphy in children. Eur J Nucl Med Mol Imaging. 2003 May;30(5):B45-50. doi: 10.1007/s00259-003-1138-9. Epub 2003 Mar 26. PMID: 12658506.

12. Bombardieri E & Giammarile F & Cumali A et al.131I/123I-Metaiodobenzylguanidine (mIBG) scintigraphy: procedure guidelines for tumor imaging. Eur J Nucl Med Mol Imaging (2010)37:2436-2446 DOI 10.1007/s00259-010-1545-7.

13. Yanik GA, Parisi MT, Shulkin BL, Naranjo A, Kreissman SG, London WB, et al. Semiquantitative mIBG scoring as a prognostic indicator in patients with stage 4 neuroblastoma: a report from the Children's Oncology Group. J Nucl Med. 2013; 54:541–8

14. Kwee TC, Takahara T, Vermoolen MA et al. Whole-body diffusion-weighted imaging for staging malignant lymphoma in children. Pediatr Radiol. 2010; 40:1592-602

15. Goo HW. Whole-body MRI of neuroblastoma. Eur J Radiol. 2010; 75: 306-314.

16. Goo HW, Choi SH, Ghim T, Moon HN, Seo JJ. Whole-body MRI of paediatric malignant tumours: comparison with conventional oncological imaging methods Pediatr Radiol. 2005; 35:766-773.

17. Pai Panandiker AS, Coleman J, Shulkin B. Whole-body pediatric neuroblastoma imaging: 123I-mIBG and beyond. Clin Nucl Med. 2015; 40:737–9

18. Ishiguchi H, Ito S, Kato K, et al. Diagnostic performance of 18F-FDG PET/CT and whole-body diffusion-weighted imaging with background body suppression (DWIBS) in detection of lymph node and bone metastases from pediatric neuroblastoma. Ann Nucl Med. 2018; 32:348-362.

19. Bar-Sever Z, Biassoni L, Shulkin B et al. Guidelines on nuclear medicine imaging in neuroblastoma. Eur J Nucl Med Mol Imaging. 2018 Oct;45(11): 2009 -2024. Doi: 10.1007/s00259-018-4070-8.

20. Lassmann M, Treves ST. Pediatric Radiopharmaceutical Administration: harmonization of the 2007 EANM Paediatric Dosage Card (Version 1.5.2008) and the 2010 North American Consensus guideline. Eur J Nucl Med Mol Imaging. 2014; 41:1636

21. Matthay KK, Shulkin B, Ladenstein R, Michon J, Giammarile F, Lewington V, Pearson AD, Cohn SL. Criteria for evaluation of disease extent by (123)I-metaiodobenzylguanidine scans in neuroblastoma: a report for the International Neuroblastoma Risk Group (INRG) Task Force. Br J Cancer. 2010; 102:1319-1326.

22. Decarolis B, Schneider C, Hero B, Simon T, Volland R, Roels F, Dietlein M, Berthold F, Schmidt M. Iodine-123 metaiodobenzylguanidine scintigraphy scoring allows prediction of outcome in patients with stage 4 neuroblastoma: results of the Cologne interscore comparison study. J Clin Oncol. 2013; 31:944-51.

23. Sharp SE1, Shulkin BL, Gelfand MJ, Salisbury S, Furman WL. 123I-MIBG scintigraphy and 18F-FDG PET in neuroblastoma.J Nucl Med. 2009; 50:1237-43.

24. Orr KE, MacHugh K . The new international neuroblastoma response criteria. Pediatr Radiol. 2019; 49:1433-1440.

25. Siegel MJ, Jaju A. MR imaging of neuroblastic masses. Magn Reson Imaging Clin N Am. 2008; 16: 499-513.

26. Ladenstein R, Potscheger U, Valteau-Couanet D et al. Investigation of the role of Dinutiximab Beta-based Immunotherapy in the SIOPEN High-Risk Neuroblastoma 1 Trial (HR-NBL1). Cancers. 2020 Jan 28; 12(2):309. Doi: 10.3390/carcers1202309.

27. Wang X, Pirasteh A, Brugarolas J, Rofsky NM, Lenkinski RE, Pedrosa I, Madhuranthakam AJ. Whole-body MRI for metastatic cancer detection using T2 -weighted imaging with fat and fluid suppression. Magn Reson Med. 2018; 80:1402-1415

28. Bohlscheid A, Nuss D, Lieser S, Busch HP. Tumorsuche mittels kernspintomografischer Diffusionsbildgebung--Erste Erfahrungen [Tumor search with diffusion-weighted imaging--first experience]. Rofo. 2008 Apr;180(4):302-9. German. doi: 10.1055/s-2008-1027228. PMID: 18370348.

29. Takahara T, Imai Y, Yamashita T, Yasuda S, Nasu S, Van Cauteren M. Diffusion weighted whole body imaging with background body signal suppression (DWIBS): technical improvement using free breathing, STIR and high resolution 3D display. Radiat Med. 2004; 22: 275-82.

30. Gahr N, Darge K, Hahn G, Kreher BW, von Buiren M, Uhl M. Diffusion-weighted MRI for differentiation of neuroblastoma and ganglioneuroblastoma/ganglioneuroma. Eur J Radiol. 2011; 79:443–6.

31. Neubauer H, Li M, Müller VR, Pabst T, Beer M. Diagnostic value of diffusion-weighted MRI for tumor characterization, differentiation and monitoring in pediatric patients with neuroblastic tumors. 2017; 189:640–50.

32. Serin HI, Gorkem SB, Doganay S, Cıracı S, Unal E, Guzel M, et al. Diffusion weighted imaging in differentiating malignant and benign neuroblastic tumors. Jpn J Radiol. 2016; 34:620–4.

33. Demir S, Altinkaya N, Kocer NE, Erbay A, Oguzkurt P. Variations in apparent diffusion coefficient values following chemotherapy in pediatric neuroblastoma. Diagn Interv Radiol. 2015; 21:184–8.

34. Jacobs F, Thierens H, Piepsz A, Bacher K, Van de Wiele C, Ham H, Dierckx RA. Optimized tracer-dependent dosage cards to obtain weight independent effective doses. Eur J Nucl Med Mol Imaging. 2005; 32:581-8.

35. Linet MS, Kim KP, Rajaraman P. Children's exposure to diagnostic medical radiation and cancer risk: epidemiologic and dosimetric considerations. Paediatr Radiol. 2009; 39: S4-26

36. Laverdière C, Liu Q, Yasui Y, Nathan PC, Gurney JG, Stovall M, Diller LR, Cheung NK, Wolden S, Robison LL, Sklar CA. Long-term outcomes in survivors of neuroblastoma: a report from the

Childhood Cancer Survivor Study. J Natl Cancer Inst. 2009 Aug 19;101(16):1131-40. doi: 10.1093/jnci/djp230. Epub 2009 Jul 31. PMID: 19648511; PMCID: PMC2728747.

37. Mostoufi-Moab S, Seidel K, Leisenring WM, et al. Endocrine abnormalities in aging survivors of childhood cancer: A report from the Childhood Cancer Survivor Study. J Clin Oncol 34:3240-3247, 2016

38. Chemaitilly W, Cohen LE, Mostoufi-Moab S, Patterson BC, Simmons JH, Meacham LR, van Santen HM, Sklar CA. Endocrine Late Effects in Childhood Cancer Survivors. J Clin Oncol. 2018 Jul 20;36(21):2153-2159. doi: 10.1200/JCO.2017.76.3268. Epub 2018 Jun 6. PMID: 29874130.

39. Ording Müller LS, Avenarius D, Olsen OE. High signal in bone marrow at diffusion-weighted imaging with body background suppression (DWIBS) in healthy children. Pediatr Radiol. 2011 Feb ; 41(2): 221−226. Doi: 10.1007/s00247-010-1774-8.

40. Kwee TC, Takahara T, Ochiai R, Nievelstein RA, Luijten PR. Diffusion-weighted whole-body imaging with background body signal suppression (DWIBS): features and potential applications in oncology Eur Radiol. 2008 Sep;18(9):1937-52.

41. Petralia G, Padhani AR, Pricolo P, Zugni F, Martinetti M, Summers PE, Grazioli L, Colagrande S, Giovagnoni A, Bellomi M; Italian Working Group on Magnetic Resonance. Whole-body magnetic resonance imaging (WB-MRI) in oncology: recommendations and key uses. Radiol Med. 2019; 124:218-233.

42. Petralia G, Padhani AR. Whole-Body Magnetic Resonance Imaging in Oncology: Uses and Indications. Magn Reson Imaging Clin N Am. 2018; 26:495-507.

Tables

Due to technical limitations the Tables are available as a download in the Supplementary Files.
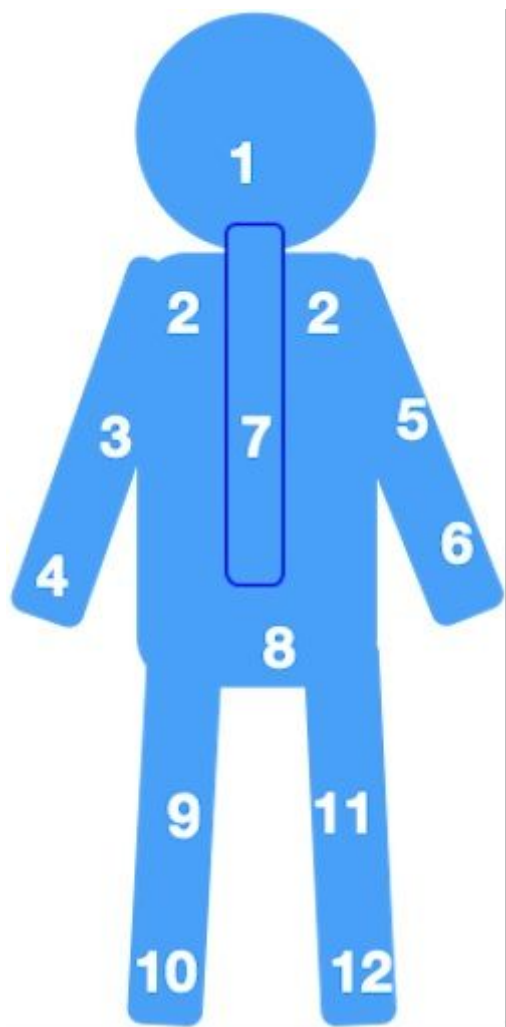
Figures

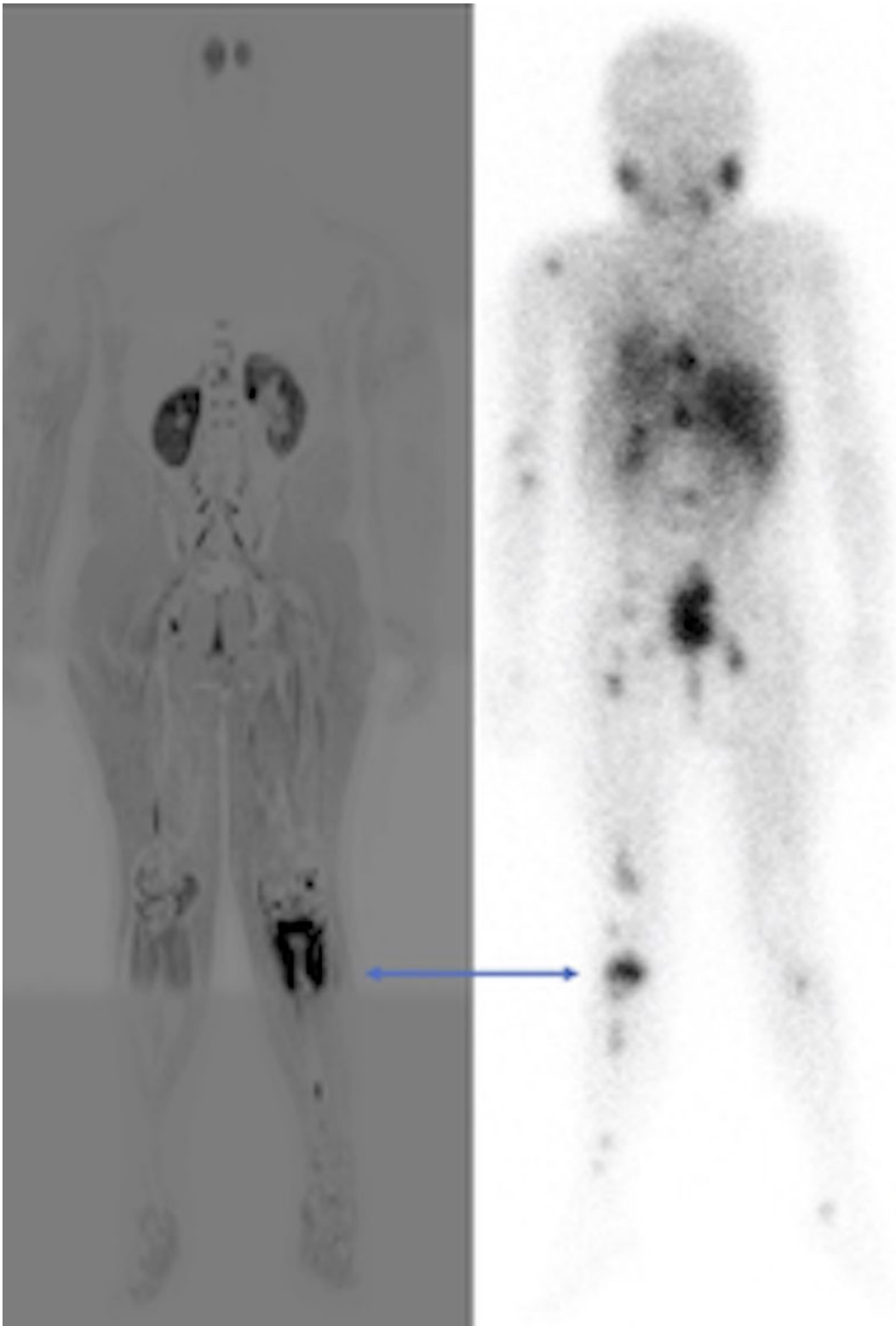**Figure 1**

Numbering of 12 segments, see Tab.1

Figure 2

Left knee intese DWIBS –WB restriction diffusion alteration and skeletal intense MIBG uptake in HR-NB, arrow
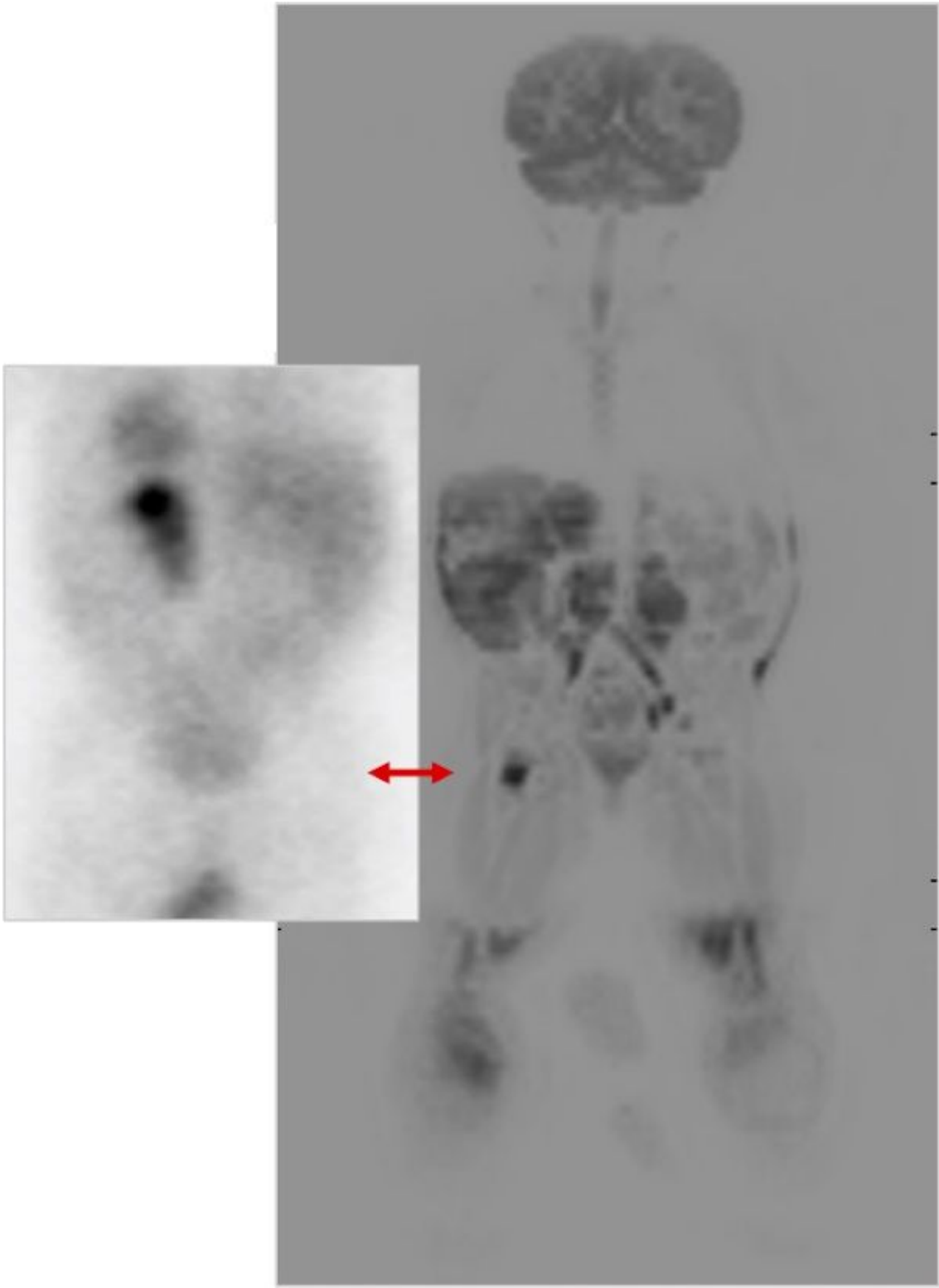
Figure 3

False positive DWIBS –WB on right proximal femur versus a negative MIBG scan, arrow
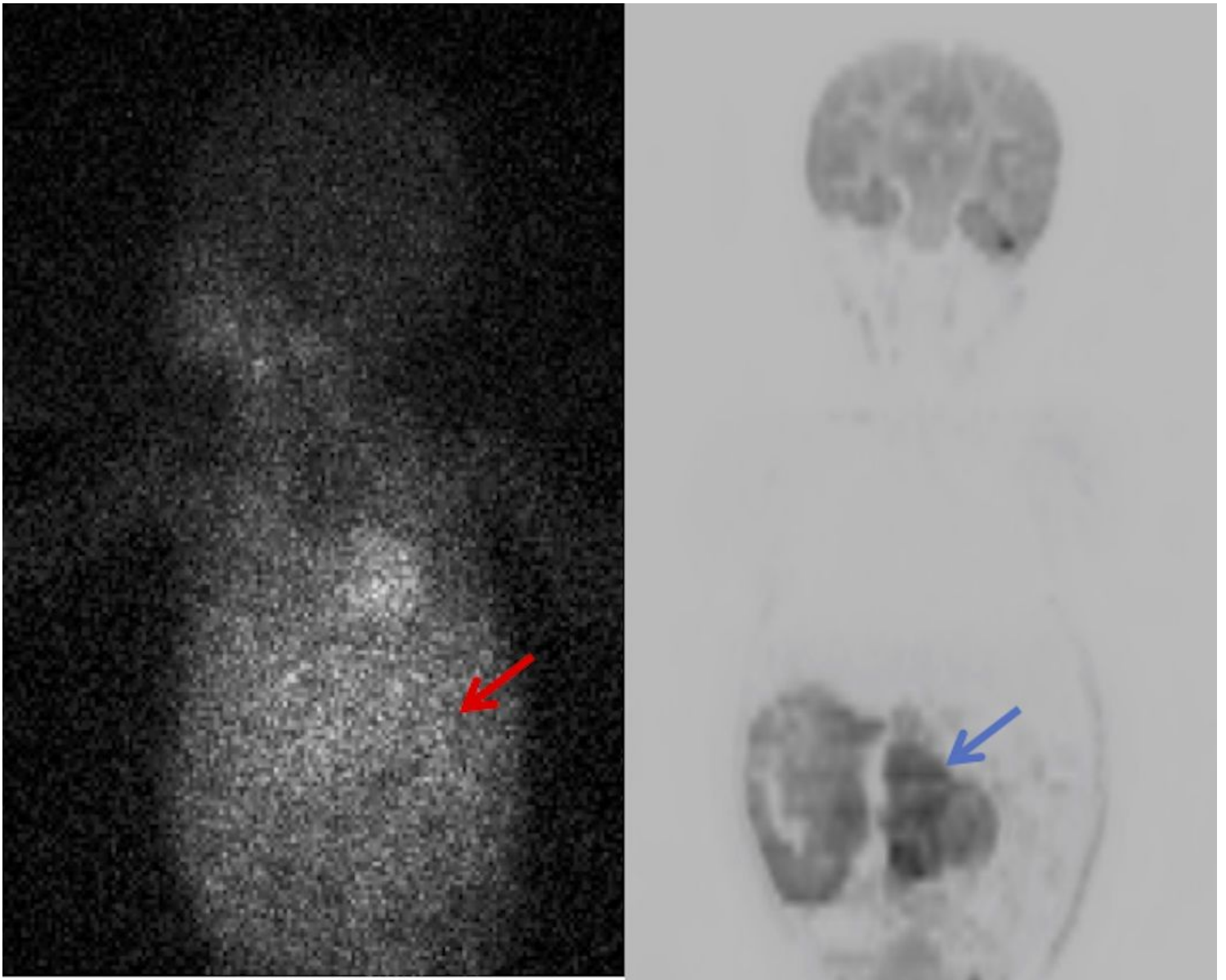
Figure 4

High DWIBS –WB restricted diffusion on a large abdominal primary tumor with a few-avid MIBG abdominal uptake in a Lines NB at staging, arrows
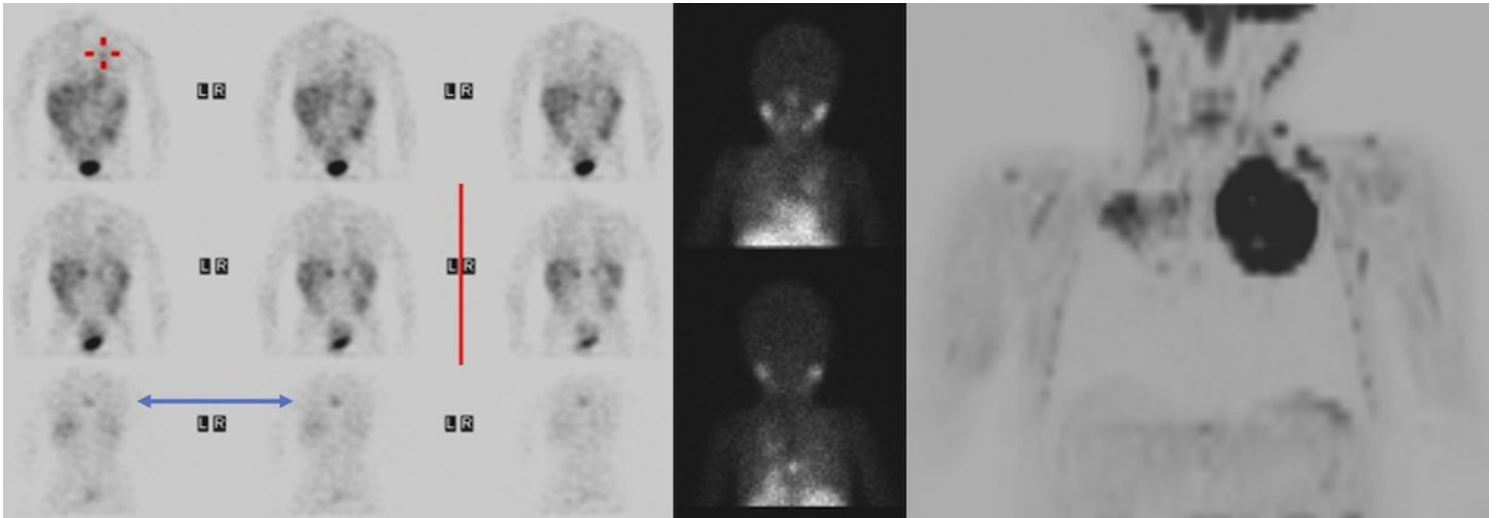
Figure 5

Large intense DWIBS −WB diffusion-restricted area on left thorax versus a mild visualization on MIBG scan, where instead is well evidenced an intense MIBG spine alteration (spinous process) arrow. Revision of whole tumor hystopatholo-gy showed a small site of NB in a big thoracic ganglioneuroblastoma with supra-clavicular benign lymphonodes

Supplementary Files

This is a list of supplementary files associated with this preprint. Click to download.

- Tables.pdf